

Vision Transformer for Contrastive Clustering

Hua-Bao Ling, Bowen Zhu, Dong Huang, *Member, IEEE*, Ding-Hua Chen,
Chang-Dong Wang, *Member, IEEE*, and Jian-Huang Lai, *Senior Member, IEEE*,

Abstract—Vision Transformer (ViT) has shown its advantages over the convolutional neural network (CNN) with its ability to capture global long-range dependencies for visual representation learning. Besides ViT, contrastive learning is another popular research topic recently. While previous contrastive learning works are mostly based on CNNs, some latest studies have attempted to jointly model the ViT and the contrastive learning for enhanced self-supervised learning. Despite the considerable progress, these combinations of ViT and contrastive learning mostly focus on the instance-level contrastiveness, which often overlook the contrastiveness of the global clustering structures and also lack the ability to directly learn the clustering result (e.g., for images). In view of this, this paper presents an end-to-end deep image clustering approach termed Vision Transformer for Contrastive Clustering (VTCC), which for the first time, to the best of our knowledge, unifies the Transformer and the contrastive learning for the image clustering task. Specifically, with two random augmentations performed on each image in a mini-batch, we utilize a ViT encoder with two weight-sharing views as the backbone to learn the representations for the augmented samples. To remedy the potential instability of the ViT, we incorporate a convolutional stem, which uses multiple stacked small convolutions instead of a big convolution in the patch projection layer, to split each augmented sample into a sequence of patches. With representations learned via the backbone, an instance projector and a cluster projector are further utilized for the instance-level contrastive learning and the global clustering structure learning, respectively. Extensive experiments on eight image datasets demonstrate the stability (during the training-from-scratch) and the superiority (in clustering performance) of VTCC over the state-of-the-art.

Index Terms—Deep clustering, Image clustering, Vision Transformer, Contrastive learning, Self-supervised learning.

I. INTRODUCTION

VISION Transformer (ViT) [1], as a promising alternative network architecture to the convolutional neural network (CNN) [2], [3], has received increasing attention recently. Although the CNN can effectively capture the local information, yet there is still a critical need to model the global long-range dependencies between image elements in various computer vision tasks. Inspired by the significant success

of the Transformer architecture that adopts the multi-head self-attention (MHSA) mechanism [4] in natural language processing (NLP), the ViT has also emerged as a pioneering direction to apply the Transformer architecture in computer vision [1]. Typically, in ViT, an input image is first split into a sequence of patches by a non-overlapping $p \times p$ convolutional operation with stride- p (e.g., with $p = 16$) and then these patches are fed into a standard Transformer encoder architecture [4] for representation learning. Following this simple yet powerful backbone architecture, many Transformer-based models have been developed and some have become the predominant architectures for a variety of vision tasks, such as image classification [1], [5], object detection [6], [7], and semantic segmentation [8].

In the meantime, self-supervised learning (SSL) [9]–[12] has gained tremendous progress in the past few years, which aims to learn visual representation from large-scale unlabeled data in a self-supervised manner. There are three mainstream categories of the self-supervised framework [13], which are generative [14], [15], contrastive [9], [10], and generative-contrastive [16] architectures. Among them, the contrastive learning has recently made some breakthroughs, which aims to “learn to compare” via an information noise contrastive estimation (InfoNCE) [17] loss function. A representative work is MoCo [10], which utilizes the momentum contrastive learning to two encoders and employs a queue to save negative samples. Another representative work is SimCLR [9], which demonstrates the importance of constructing the samples pairs by various data augmentations. Besides this, SimCLR can be trained with a large batch size instead of the momentum contrast in MoCo.

Rapid progresses have been made in both the Transformer-based architectures and the contrastive learning architectures. However, these two types of architectures are mostly developed independently and almost all contrastive learning backbones are based on the CNN. It has been a crucial question whether the ViT backbone can provide better representation learning for contrastive learning than CNN. Recently, some research works have attempted to exploit the advantages of both of them. For example, Chen et al. [18] investigated the instability on training self-supervised ViT. Caron et al. [19] explored some emerging properties of the self-supervised ViT. A more recent development of the contrastive learning is its combination with the image clustering task. Typically, Li et al. [20] utilized the contrastive learning at the instance-level and the cluster-level for simultaneous representation learning and image clustering, where the CNN is adopted as the backbone. As the CNN is more focused on the local information, it is intuitive that the investigation of the global dependencies in the image via Transformer may also provide rich information

This project was supported by the NSFC (61976097, 61876193 & 62076258) and the Natural Science Foundation of Guangdong Province (2021A1515012203). (*Corresponding author: Dong Huang*)

H.-B. Ling, B. Zhu, D. Huang, and D.-H. Chen are with the College of Mathematics and Informatics, South China Agricultural University, Guangzhou, China.

E-mail: hbling@stu.scau.edu.cn, bowenzhu0329@hotmail.com, huangdonghere@gmail.com, dhchen@stu.scau.edu.cn.

C.-D. Wang and J.-H. Lai are with the School of Computer Science and Engineering, Sun Yat-sen University, Guangzhou, China, and also with Guangdong Key Laboratory of Information Security Technology, Guangzhou, China, and also with Key Laboratory of Machine Intelligence and Advanced Computing, Ministry of Education, China.

E-mail: changdongwang@hotmail.com, sts1jh@mail.sysu.edu.cn.

H.-B. Ling and B. Zhu contribute equally to this work.

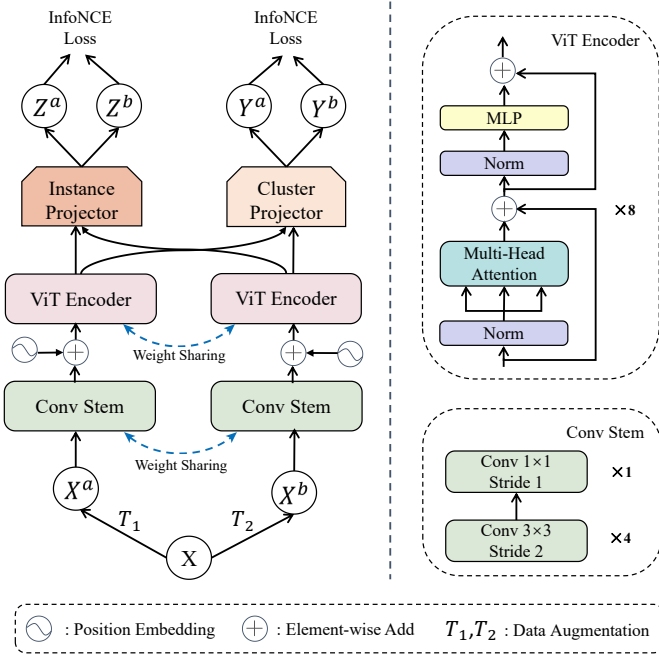


Fig. 1. Vision Transformer for Contrastive Clustering (VTCC).

to enhance the image clustering performance, especially for complex images. Yet it remains an unaddressed problem how to effectively leverage the Transformer (or ViT) in collaboration with the contrastive learning for enhanced representation learning and clustering of highly complex images.

This paper for the first time, to the best of our knowledge, unifies the ViT and the contrastive learning for deep image clustering. To make this unification possible and practical, some critical challenges should be addressed. Different from the CNN [2], [3], the training recipes for ViT are sensitive, especially in the self-supervised scenarios [18], which involve the choice of hyper-parameters, the number of encoder blocks, and so forth. As a consequence, the training of ViT usually needs a large dataset, and the instability issue is often encountered [19], [21], [22]. Recently, some research works suggest that this issue arises from the patch projection layer in the standard ViT and attempt to solve it from different perspectives [18], [22]. For example, Chen et al. [18] alleviated the instability issue by simply freezing the patchify stem instead of using the random initialization patch projection layer. Further, Xiao et al. [22] proposed a simple approach by replacing the origin patchify stem with a convolutional stem, which is implemented by a small number of stacked stride-2 3 convolutions in the patch projection layer. In this work, we surprisingly find that the use of multiple stacked small convolutions instead of a big convolution in the patch projection layer, which to some extent resembles the typical design of CNNs [2], [3], can significantly benefit the contrastive image clustering with Transformer, even for some relative small datasets.

Specifically, we propose a novel deep clustering approach termed Vision Transformer for Contrastive Clustering (VTCC) (as illustrated in Fig. 1). To remedy the potential instability, a convolutional stem layer with multiple stacked

small-size convolutions is incorporated to split an augmented sample image into a sequence of patches. With two random augmentations performed on each image to obtain two augmented samples, we feed the sequences of patch vectors of the augmented samples to the backbone, which encompasses two weight-sharing views in a standard Transformer encoder architecture. With the representations of the augmented samples learned with the self-attention mechanism in the backbone, the contrastive learning is enforced via an instance projector and a cluster projector, which simultaneously explore the instance contrastiveness and the global clustering structures. Notably, the Transformer backbone with convolutional stem and the two contrastive projectors in our VTCC framework are jointly trained in an end-to-end manner. Extensive experiments are conducted on eight challenging image datasets, which confirm the benefits brought in by the Transformer and demonstrate the stability (during the training-from-scratch) and the superior clustering performance of VTCC in comparison with the state-of-the-art.

For clarity, the main contributions of this work are summarized as follows:

- This paper makes the first attempt (to our knowledge) to effectively bridge the gap between the Transformer and the contrastive learning for the deep image clustering task, with the global dependencies, the instance contrastiveness, and the clustering structure learning jointly modeled.
- This paper reveals the importance of the convolutional stem via multiple stacked small convolutions in the patch projection layer, which improves the stability during the ViT training from scratch for image clustering on small datasets.
- This paper presents an end-to-end deep clustering approach termed VTCC based on ViT and contrastive learning. Experimental results on eight real-world image datasets have confirmed the promising capability of Transformer for the clustering of complex images and the advantages of VTCC over the state-of-the-art deep clustering approaches.

The remainder of the paper is organized as follows. The proposed VTCC approach is described in Section II. The experimental results and analysis are provided in Section III, which is followed by the conclusion in Section IV.

II. PROPOSED FRAMEWORK

In this section, we describe the details of our VTCC approach. First, an overview of the network architecture is given in Section II-A. Then the ViT backbone is presented in Section II-B. Finally, the overall loss function of VTCC is provided in Section II-C.

A. Network Architecture

The architecture of VTCC is illustrated in Fig. 1, which consists of three main components, namely, a ViT backbone with two weight-sharing views to extract feature representations for augmented samples, an instance-level contrastive learning module to maximize the similarity of positive pairs,

and a global clustering structure learning module that achieves the soft label prediction for image clustering.

Specifically, for each image in a mini-batch of N images, two data augmentations are randomly selected with a certain probability, which is the common practice in contrastive learning [9], [10]. Then the augmented samples are split into fixed-size patches by the convolutional stem [22], which will be described in Section II-B1. With each sample divided into a sequence of patches and embedded by linear projection, a standard Transformer encoder is utilized for learning the feature representations, which are then fed to two projectors, i.e., the instance projector and the cluster projector, for instance-level contrastive learning and global clustering structure learning, respectively. Finally, the overall network is trained by two contrastive loss functions in an end-to-end manner and the clustering result can thus be obtained. Additionally, the pseudo-code of VTCC is presented in Algorithm 1.

Algorithm 1: VTCC: A PyTorch-like Pseudo Code

```

#  $f(\cdot)$  : Vision Transformer
#  $g_I(\cdot)$  : Instance projector
#  $g_C(\cdot)$  : Cluster projector
#  $InfoNCE(\cdot, \cdot)$  : InfoNCE loss
#  $InsLoss(\cdot, \cdot)$  : Instance-level contrastive loss
#  $CluLoss(\cdot, \cdot)$  : Cluster-level contrastive loss
#  $T_1, T_2$  : Augmentations selected from family  $T$ 
for x in loader: # Load a mini-batch  $x$  with  $N$  samples
    # Obtain augmented views of  $x$ 
     $x_1, x_2 = T_1(x), T_2(x)$ 
    # Extract feature embeddings
     $h_1, h_2 = f(x_1), f(x_2)$ 
    # Map embeddings to subspace via  $g_I$ 
     $z_1, z_2 = g_I(h_1), g_I(h_2)$ 
    # Map embeddings to subspace via  $g_C$ 
     $c_1, c_2 = g_C(h_1), g_C(h_2)$ 

    # Loss calculation
     $loss = InsLoss(z_1, z_2) + CluLoss(c_1, c_2)$ 
     $loss.backward()$ 

     $update(f)$  # Optimize the parameters of  $f$ 

def  $InsLoss(z_1, z_2)$ :
    return  $(InfoNCE(z_1, z_2) + InfoNCE(z_2, z_1))/2$ 
def  $CluLoss(c_1, c_2)$ :
    return  $(InfoNCE(c_1, c_2) + InfoNCE(c_2, c_1))/2$ 

```

B. Backbone with Vision Transformer

Unlike the CNNs which can be performed on the sample image directly, a Transformer encoder requires a sequence of vectors as input. In VTCC, we utilize a convolutional stem with multiple stacked small-size convolutions to split each augmented sample into fix-size patches, which are then fed to a standard ViT [1] as the backbone. In the following, we will describe the convolutional stem and the Transformer

encoder representation learning in Sections II-B1 and II-B2, respectively.

1) *Convolutional Stem*: To convert a 2D image to a 1D sequence of feature embedding, a conventional strategy adopted in ViT is to apply a $p \times p$ convolution operation with a stride p to the input image (typically with $p = 16$), which is referred to as the patchify stem. It captures a lot of non-overlapping patches with $p \times p$ size, and then flatten these patches to form the input sequence for the Transformer encoder. However, this type of convolution operation with a large convolution kernel and a large stride runs counter to the classical convolution setting in the general neural networks [2] which usually adopt some small-size (e.g. 3×3) convolution kernels. In view of this, Xiao et al. [22] proposed a *convolutional stem* which replaces the patchify stem in the original ViT model by a small number of stacked stride-2, 3×3 convolutions. Empirically, using the convolutional stem on the ViT patch embedding layer is particularly beneficial for our image clustering task (as evaluated in Section III-D).

Specifically, to obtain the 1D image sequence, we first incorporate four blocks in the convolutional stem, where each block includes a standard convolution operation with stride-2, 3×3 convolution kernel, followed by a batch normalization and a ReLU activation function (as shown in Fig. 1). Due to the Transformer encoder requires the 1D image sequence as input, we use a single 1×1 convolution to match the input dimension of the Transformer encoder. In practice, compared with the large convolution, using multiple small convolutions may capture the fine-grained local features which is more conducive to the representation learning and thus gives rise to better stability and clustering performance.

2) *Transformer Encoder*: Various scales of ViT models have been devised in previous works. In this paper, we adopt the ViT-Small [23] as the backbone which provides effective representation learning capability while maintaining high efficiency.

Specifically, based on the input sequence of patches embedding, each encoder layer is built upon the standard Transformer architecture which consists of a multi-head self-attention and a MLP block. In addition, a layer-norm operation is adopted before each block, and residual connections after each block. Here, the Transformer encoder applies the self-attention layers to model global relations between input embeddings, which exhibits an advantage over the CNNs where the receptive field of convolutional kernels are limited locally. However, the Transformer architecture is permutation-invariant theoretically, which may overlook the rich information of relative positions. Therefore, we also incorporate the position encodings [4] to the input sequence of each self-attention layer.

C. Loss Function

To achieve the instance-level and cluster-level self-supervision, we utilize two independent projectors which have the same MLP structure but different parameters for mapping the feature embeddings learned by the backbone network to different subspaces (i.e., the instance subspace and the cluster subspace). By means of these two projectors, the instance-level

contrastive learning and cluster-level contrastive learning are respectively enforced.

1) *Instance-level Contrastive Learning*: The purpose of the instance-level contrastive learning is to maximize the similarity between two different augmentation views of the same input image by pulling closer the distance between a positive pair in the instance subspace while pushing away the embeddings of the negative pairs. Let x_i^a and x_i^b denote the two augmented samples for the input image x_i , and h_i^a and h_i^b denote the feature embeddings of x_i^a and x_i^b , respectively, learned by the backbone. Since directly using the feature embeddings h_i^a and h_i^b for similarity calculation may lead to the loss of information [9], we utilize an instance projector with a three-layer MLP, which is denoted as g_I and maps the embeddings h_i^a and h_i^b to a low-dimensional subspace, leading to $Z_i^a = g_I(h_i^a)$ and $Z_i^b = g_I(h_i^b)$, respectively. Then, the cosine similarity is used to measure the pair-wise similarity, that is

$$s(\alpha, \beta) = \frac{\alpha^\top \beta}{\|\alpha\| \cdot \|\beta\|}, \quad (1)$$

where α and β are two feature vectors with the same dimension. Given a sample image x_i , the similarity between its low-dimensional embeddings of two augmented views (i.e., Z_i^a and Z_i^b) is calculated as $s(Z_i^a, Z_i^b)$. Thereby, the instance-level contrastive loss [17] for the input image x_i is defined as

$$l_i = l_i^a + l_i^b, \quad (2)$$

with

$$l_i^a = -\log \frac{\exp(s(Z_i^a, Z_i^b)/\tau_I)}{\sum_{j=1, j \neq i}^N [\exp(s(Z_i^a, Z_j^a)/\tau_I) + \exp(s(Z_i^a, Z_j^b)/\tau_I)]} \quad (3)$$

and

$$l_i^b = -\log \frac{\exp(s(Z_i^b, Z_i^a)/\tau_I)}{\sum_{j=1, j \neq i}^N [\exp(s(Z_i^b, Z_j^b)/\tau_I) + \exp(s(Z_i^b, Z_j^a)/\tau_I)]}, \quad (4)$$

where τ_I is the temperature parameter, N is the size of the mini-batch, and l_i^a and l_i^b are the instance-level contrastive losses for the augmented samples x_i^a and x_i^b , respectively. Finally, the instance-level contrastive loss for a mini-batch of N input images is defined as [9]

$$L_{ins} = \frac{\sum_{i=1}^N l_i}{2N}. \quad (5)$$

By optimizing the loss function (5), the network can be trained by maximizing the similarity between the low-dimensional embeddings of the augmented sample pairs from the same input image (i.e., the positive pairs), while minimizing the similarity between the embeddings of the augmented sample pairs from different input images (i.e., the negative pairs).

2) *Global Clustering Structure Learning*: Besides instance-level contrastive loss, we proceed to define the cluster-level contrastive loss for global clustering structure learning. It aims to maximize the similarity of the positive cluster pairs while minimizing the similarity of the negative cluster pairs. Similar to the instance projector, we utilize a cluster projector with a three-layer MLP and a softmax layer, denoted as

g_C , to map the feature embeddings to the low-dimensional subspace, leading to $Y_i^a = g_C(h_i^a)$ and $Y_i^b = g_C(h_i^b)$. With a softmax layer (of dimension K) added to the end of the cluster projector, the output of the cluster projector Y_i^a can be regarded as the cluster distribution for the first augmented view of the input image x_i (and Y_i^b for the second augmented view of x_i). For a mini-batch of N input images, we can obtain the representation matrices $Y^a \in \mathbb{R}^{N \times K}$ and $Y^b \in \mathbb{R}^{N \times K}$ for the two augmented views by stacking the feature representations of the N samples, where the i -th column (denoted as \hat{Y}_i^k with $k \in \{a, b\}$) of each of these two matrices indicates the probability of allocating each sample to the i -th cluster. Thereby, for any $i, j \in [1, K]$, the cluster \hat{Y}_i^a and the cluster \hat{Y}_j^a form a positive cluster pair if $i = j$ and a negative cluster pair if $i \neq j$.

By using the cosine similarity (1) to measure the similarity between the cluster distributions, the contrastive loss for the i -th cluster is defined as

$$\hat{l}_i = \hat{l}_i^a + \hat{l}_i^b, \quad (6)$$

with

$$\hat{l}_i^a = -\log \frac{\exp(s(\hat{Y}_i^a, \hat{Y}_i^b)/\tau_C)}{\sum_{j=1, j \neq i}^K [\exp(s(\hat{Y}_i^a, \hat{Y}_j^a)/\tau_C) + \exp(s(\hat{Y}_i^a, \hat{Y}_j^b)/\tau_C)]} \quad (7)$$

and

$$\hat{l}_i^b = -\log \frac{\exp(s(\hat{Y}_i^b, \hat{Y}_i^a)/\tau_C)}{\sum_{j=1, j \neq i}^K [\exp(s(\hat{Y}_i^b, \hat{Y}_j^b)/\tau_C) + \exp(s(\hat{Y}_i^b, \hat{Y}_j^a)/\tau_C)]}, \quad (8)$$

where τ_C is the temperature parameter, and \hat{l}_i^a and \hat{l}_i^b are the cluster-level contrastive losses of the i -th cluster in the first view and the second view, respectively. Finally, the cluster-level contrastive loss for the K clusters is defined as [20]

$$L_{clu} = \frac{1}{2K} \sum_{i=1}^K \hat{l}_i - Entropy(p(Y^a)) - Entropy(p(Y^b)). \quad (9)$$

To avoid the trivial solution that assigns most samples to a single cluster, the entropy term is incorporated to the loss function, which is defined as

$$Entropy(p(Y^k)) = -\sum_{i=1}^K [p(\hat{Y}_i^k) \log p(\hat{Y}_i^k)], \quad (10)$$

$$p(\hat{Y}_i^k) = \frac{\sum_{j=1}^N y_{ji}^k}{\|\hat{Y}_i^k\|_1}, \text{ for } k \in \{a, b\}, \quad (11)$$

where y_{ji}^a (or y_{ji}^b) denotes the entry in the j -th row and the i -th column of the representation matrix Y^a (or Y^b).

3) *Overall Loss Function*: In VTCC, we jointly optimize the losses L_{ins} and L_{clu} to enforce the instance-level and cluster-level contrastive learning and obtain the clustering result. Therefore, the overall loss function is defined as

$$L_{total} = L_{ins} + L_{clu}. \quad (12)$$



Fig. 2. Some examples of the eight image datasets.

III. EXPERIMENTS

In this section, we conduct experiments on eight real-world image datasets to evaluate the proposed VTCC approach against the state-of-the-art deep clustering approaches. First, we describe the implementation details in Section III-A. Then we summarize the datasets and the evaluation metrics in Section III-B. Further, the quantitative comparison is given in Section III-C. Finally, the contributions of different components in VTCC are evaluated in Section III-D.

A. Implementation Details

In this work, we follow the setting of data augmentations in BYOL [11] and use the Adam optimizer with the initial learning rate of 0.0003. For the ViT architecture, we adopt the designs in the origin ViT. In the experiments, we utilize a lightweight version of ViT, i.e., ViT-Small [23], as our backbone with a dimension size of 384 and 8 blocks of encoder layers. For a fair comparison, we use a 224×224 image size, and adopt four small 3×3 convolutions instead of a large 16×16 convolution, followed by 1×1 convolution in convolutional stem. Each of the projectors uses a three-layer MLP, which follows the practice of MoCov3 [18]. We train our VTCC model from scratch for 1,000 epochs with a batch size of 128. All experiments are conducted on a single NVIDIA RTX 3090 GPU and CUDA 11.0.

B. Datasets and Evaluation Metrics

In our experiments, eight real-world image datasets are used for evaluation, including RSOD [24], UC-Merced [25], SIRI-WHU [26], AID [27], D0 [28], DTD [29], Chaoyang [30], and

TABLE I
THE IMAGE DATASETS USED IN OUR EXPERIMENTS.

Dataset	#Samples	#Classes
RSOD [24]	976	4
UC-Merced [25]	2,100	21
SIRI-WHU [26]	2,400	12
AID [27]	10,000	30
D0 [28]	4,508	40
DTD [29]	5,640	47
Chaoyang [30]	6,160	4
CIFAR-100 [31]	60,000	20

CIFAR-100 [31]. For CIFAR-100, we use its 20 super-classes as the ground-truth. For clarity, we summarize the statistics of each dataset in Table I and illustrate some sample images of each dataset in Fig. 2.

Following the standard evaluation protocol in image clustering, we adopt three widely-used evaluation metrics in the experiments, including the normalized mutual information (NMI) [32], the accuracy (ACC) [33], and the adjusted Rand index (ARI) [34]. Note that higher values of these metrics indicate better clustering results.

C. Comparisons with State-of-the-Art methods

In this section, we evaluate the performance of the proposed VTCC method against twelve baseline clustering methods, including seven traditional clustering methods and five deep clustering methods. The seven traditional clustering methods include K -means [35], SC [36], AC [37], NMF [38], PCA [39], BIRCH [40], GMM [41], and the five deep clustering

TABLE II
THE NMI SCORES OF DIFFERENT IMAGE CLUSTERING METHODS ON EIGHT DATASETS.

Dataset	RSOD	UC-Merced	SIRI-WHU	AID	D0	DTD	Chaoyang	CIFAR-100
<i>K</i> -means	0.162	0.204	0.145	0.209	0.299	0.119	0.024	0.083
SC	0.146	0.211	0.161	0.189	0.305	0.118	0.022	0.090
AC	0.168	0.214	0.166	0.204	0.319	0.125	0.026	0.098
NMF	0.176	0.202	0.245	0.193	0.255	0.127	0.018	0.076
PCA	0.163	0.206	0.164	0.216	0.308	0.124	0.024	0.084
BIRCH	0.148	0.225	0.162	0.204	0.315	0.123	0.026	-
GMM	0.160	0.198	0.160	0.205	0.289	0.120	0.024	0.084
DEC	0.296	0.120	0.183	0.217	0.328	0.128	0.001	0.101
IDEC	0.209	0.119	0.178	0.207	0.309	0.128	0.001	0.103
ASPC-DA	0.054	0.137	0.103	0.060	0.153	0.084	0.026	-
IDFD	0.391	0.572	0.540	0.696	0.663	0.410	0.309	0.428
CC	0.457	0.609	0.603	0.752	0.693	0.480	0.365	0.424
VTCC(Ours)	0.611	0.658	0.693	0.794	0.753	0.487	0.373	0.432

TABLE III
THE ACC SCORES OF DIFFERENT IMAGE CLUSTERING METHODS ON EIGHT DATASETS.

Dataset	RSOD	UC-Merced	SIRI-WHU	AID	D0	DTD	Chaoyang	CIFAR-100
<i>K</i> -means	0.388	0.200	0.229	0.163	0.204	0.090	0.320	0.137
SC	0.425	0.183	0.210	0.123	0.195	0.091	0.312	0.136
AC	0.371	0.188	0.222	0.151	0.209	0.091	0.329	0.138
NMF	0.420	0.208	0.275	0.161	0.187	0.091	0.305	0.127
PCA	0.388	0.198	0.227	0.173	0.220	0.090	0.320	0.139
BIRCH	0.396	0.202	0.222	0.147	0.205	0.092	0.329	-
GMM	0.382	0.193	0.239	0.169	0.189	0.091	0.318	0.132
DEC	0.534	0.147	0.257	0.185	0.232	0.092	0.421	0.157
IDEC	0.458	0.141	0.255	0.192	0.213	0.094	0.424	0.160
ASPC-DA	0.464	0.073	0.183	0.079	0.107	0.067	0.325	-
IDFD	0.595	0.456	0.545	0.628	0.507	0.306	0.512	0.424
CC	0.538	0.480	0.604	0.622	0.511	0.358	0.575	0.426
VTCC(Ours)	0.572	0.553	0.670	0.716	0.575	0.393	0.585	0.455

TABLE IV
THE ARI SCORES OF DIFFERENT IMAGE CLUSTERING METHODS ON EIGHT DATASETS.

Dataset	RSOD	UC-Merced	SIRI-WHU	AID	D0	DTD	Chaoyang	CIFAR-100
<i>K</i> -means	0.075	0.065	0.053	0.051	0.080	0.016	0.017	0.028
SC	0.096	0.038	0.041	0.029	0.039	0.012	0.005	0.022
AC	0.071	0.057	0.057	0.048	0.080	0.015	0.010	0.034
NMF	0.052	0.089	0.118	0.056	0.068	0.017	0.002	0.023
PCA	0.075	0.064	0.063	0.054	0.088	0.015	0.017	0.029
BIRCH	0.068	0.066	0.049	0.046	0.080	0.016	0.010	-
GMM	0.069	0.062	0.062	0.053	0.074	0.015	0.016	0.028
DEC	0.325	0.053	0.083	0.075	0.105	0.017	0.006	0.039
IDEC	0.144	0.042	0.079	0.073	0.093	0.017	-	0.042
ASPC-DA	0.005	0.002	0.035	0.014	0.021	0.005	0.005	-
IDFD	0.362	0.354	0.389	0.547	0.439	0.174	0.259	0.276
CC	0.371	0.356	0.450	0.550	0.423	0.205	0.343	0.267
VTCC(Ours)	0.482	0.453	0.554	0.622	0.509	0.233	0.351	0.281

TABLE V
THE INFLUENCE OF THE CONVOLUTIONAL STEM.

Dataset	Split method	NMI	ACC	ARI
RSOD	Patchify Stem	0.570	0.565	0.461
	Convolutional Stem	0.611	0.572	0.482
Chaoyang	Patchify Stem	0.365	0.573	0.336
	Convolutional Stem	0.373	0.585	0.351

methods include DEC [42], IDEC [43], ASPC-DA [44], IDFD [45], and CC [20]. For PCA, the clustering result is obtained

by conducting *K*-means on the dimension-reduced features. For each test method, the number of clusters is set to the true number of classes of the dataset. The experimental results in terms of NMI, ACC, and ARI of different clustering methods are reported in Tables II, III, and IV, respectively.

In terms of NMI, as shown in Table II, our VTCC method consistently outperforms the baseline methods on all the eight datasets. Especially, on RSOD dataset, VTCC achieves an NMI of 0.611, while the second best method (i.e., the CC method) only obtains an NMI of 0.457, where a relative gain of 33.7% is observed. It's worth noting that the RSOD

TABLE VI
THE INFLUENCE OF ViT ARCHITECTURE.

Dataset	Model	Dimension	#Blocks	#Heads	NMI	ACC	ARI
RSOD	ViT-Tiny	192	4	12	0.557	0.563	0.454
	ViT-Small	384	8	12	0.611	0.572	0.482
	ViT-Base	768	12	12	0.480	0.554	0.393
Chaoyang	ViT-Tiny	192	4	12	0.340	0.580	0.328
	ViT-Small	384	8	12	0.373	0.585	0.351
	ViT-Base	768	12	12	0.362	0.571	0.332

TABLE VII
THE INFLUENCE OF TWO CONTRASTIVE PROJECTORS.

Dataset	Contrastive projectors	NMI	ACC	ARI
RSOD	Instance projector only	0.465	0.628	0.362
	Cluster projector only	0.529	0.618	0.425
	Instance projector + Cluster projector	0.611	0.572	0.482
Chaoyang	Instance projector only	0.343	0.478	0.240
	Cluster projector only	0.310	0.546	0.279
	Instance projector + Cluster projector	0.373	0.585	0.351

dataset is a small dataset with only 976 samples and our VTCC model is trained from scratch. As for the other bigger dataset, our VTCC method also exhibits better or significantly better clustering performance than the other deep and non-deep clustering methods. In terms of ACC and ARI, as shown in Tables III and IV, similar advantages of VTCC can be revealed in comparison with the other clustering methods. The experimental results demonstrate the superiority of our VTCC method with Transformer encoder and contrastive learning integrated for the clustering of complex images.

D. Ablation Study

In this section, we experimentally analyze the influence of different components in VTCC, including the convolutional stem, the ViT architecture, and the contrastive projectors, on the RSOD and Chaoyang datasets.

1) *Influence of Convolutional Stem*: This section conducts experiments to evaluate the influence of the convolutional stem, which is described in Section II-B1. As shown in Table V, using convolutional stem leads to an NMI score 0.611 on the RSOD dataset and 0.373 on the Chaoyang dataset, both of which are better than that of using the original patchify stem in ViT. Similar advantages in terms of ACC and ARI can also be observed, which confirm that the use of the convolutional stem is beneficial to the clustering performance of VTCC.

2) *Influence of Vision Transformer Architecture*: To evaluate the influence of the ViT architecture, we compare the performances of VTCC with different scales of Transformer encoder architectures, including ViT-Tiny [23], ViT-Small [23], and ViT-Base [23], and report the clustering results in Table VI. As shown in Table VI, on the small dataset of RSOD, ViT-Small and ViT-Tiny outperform ViT-Base, probably due to the fact that ViT-Base is the largest model (among the three) and may lead to over-fitting on the small dataset. Empirically,

the ViT-Small is a suitable choice with sufficient representation learning capability while maintaining high efficiency.

3) *Influence of Contrastive Projectors*: This section conducts experiments to evaluate the influence of the two contrastive projectors in VTCC. When testing the performance of the instance projector, the cluster projector is removed and the K -means is performed on the representation learned by the instance projector. As shown in Table VII, as for the RSOD dataset, only using the instance projector leads to an NMI of 0.465, whereas only using the cluster projector leads to an NMI of 0.529, both of which are lower than the NMI of jointly using two projectors, that is, 0.611. Although only using the instance projector can lead to a better ACC score than using both projectors, yet using both projectors yields the best performance in terms of the other two metrics on RSOD and in terms of all the three metrics on Chaoyang, which show that the joint use of two projectors mostly contribute to better clustering robustness.

IV. CONCLUSION

In this paper, a novel novel deep clustering approach termed VTCC is proposed, which unifies the ViT and the contrastive learning for the image clustering task. Specifically, we utilize a ViT encoder architecture as the backbone to extract the feature embeddings of two augmentation views, where a convolutional stem is used to split the augmented sample into a sequence of patches for the Transformer encoder. Two contrastive projectors are incorporated to enforce the instance-level contrastive learning and the global clustering structure learning simultaneously. Extensive experiments are conducted on eight real-world datasets, which have shown the superiority of VTCC over the state-of-the-art deep clustering approaches. Particularly, the experimental results reveal the benefits of Transformer for image clustering, especially for

images with complex structures. Also, we think that there is a promising potential for image clustering via Transformers and contrastive learning, where more Transformer models and network architectures can be further investigated.

REFERENCES

- [1] A. Dosovitskiy, L. Beyer, A. Kolesnikov, D. Weissenborn, X. Zhai, T. Unterthiner, M. Dehghani, M. Minderer, G. Heigold, S. Gelly, J. Uszkoreit, and N. Houlsby, "An image is worth 16x16 words: Transformers for image recognition at scale," in *Proc. of International Conference on Learning Representations (ICLR)*, 2021.
- [2] K. He, X. Zhang, S. Ren, and J. Sun, "Deep residual learning for image recognition," in *Proc. of IEEE Conference on Computer Vision and Pattern Recognition (CVPR)*, 2016.
- [3] M. Tan and Q. Le, "Efficientnet: Rethinking model scaling for convolutional neural networks," in *Proc. of International Conference on Machine Learning (ICML)*, 2019.
- [4] A. Vaswani, N. Shazeer, N. Parmar, J. Uszkoreit, L. Jones, A. N. Gomez, L. Kaiser, and I. Polosukhin, "Attention is all you need," in *Advanced in Neural Information Processing Systems (NeurIPS)*, 2017.
- [5] Z. Liu, Y. Lin, Y. Cao, H. Hu, Y. Wei, Z. Zhang, S. Lin, and B. Guo, "Swin transformer: Hierarchical vision transformer using shifted windows," in *Proc. of IEEE/CVF International Conference on Computer Vision (ICCV)*, 2021.
- [6] N. Carion, F. Massa, G. Synnaeve, N. Usunier, A. Kirillov, and S. Zagoruyko, "End-to-end object detection with transformers," in *Proc. of European Conference on Computer Vision (ECCV)*, 2020.
- [7] X. Zhu, W. Su, L. Lu, B. Li, X. Wang, and J. Dai, "Deformable detr: Deformable transformers for end-to-end object detection," *arXiv preprint arXiv:2010.04159*, 2020.
- [8] R. Strudel, R. Garcia, I. Laptev, and C. Schmid, "Segmenter: Transformer for semantic segmentation," in *Proc. of IEEE/CVF International Conference on Computer Vision (ICCV)*, 2021.
- [9] T. Chen, S. Kornblith, M. Norouzi, and G. Hinton, "A simple framework for contrastive learning of visual representations," in *Proc. of International Conference on Machine Learning (ICML)*, 2020.
- [10] K. He, H. Fan, Y. Wu, S. Xie, and R. Girshick, "Momentum contrast for unsupervised visual representation learning," in *Proc. of IEEE/CVF Conference on Computer Vision and Pattern Recognition (CVPR)*, 2020.
- [11] J.-B. Grill, F. Strub, F. Altché, C. Tallec, P. Richemond, E. Buchatskaya, C. Doersch, B. Avila Pires, Z. Guo, M. Gheshlaghi Azar *et al.*, "Bootstrap your own latent—a new approach to self-supervised learning," in *Advanced in Neural Information Processing Systems (NeurIPS)*, 2020.
- [12] M. Caron, I. Misra, J. Mairal, P. Goyal, P. Bojanowski, and A. Joulin, "Unsupervised learning of visual features by contrasting cluster assignments," in *Advanced in Neural Information Processing Systems (NeurIPS)*, 2020.
- [13] X. Liu, F. Zhang, Z. Hou, L. Mian, Z. Wang, J. Zhang, and J. Tang, "Self-supervised learning: Generative or contrastive," *IEEE Transactions on Knowledge and Data Engineering*, 2021.
- [14] A. Van den Oord, N. Kalchbrenner, L. Espeholt, O. Vinyals, A. Graves *et al.*, "Conditional image generation with PixelCNN decoders," in *Advanced in Neural Information Processing Systems (NeurIPS)*, 2016.
- [15] A. Van Oord, N. Kalchbrenner, and K. Kavukcuoglu, "Pixel recurrent neural networks," in *Proc. of International Conference on Machine Learning (ICML)*, 2016.
- [16] A. Radford, L. Metz, and S. Chintala, "Unsupervised representation learning with deep convolutional generative adversarial networks," *arXiv preprint arXiv:1511.06434*, 2015.
- [17] A. v. d. Oord, Y. Li, and O. Vinyals, "Representation learning with contrastive predictive coding," *arXiv preprint arXiv:1807.03748*, 2018.
- [18] X. Chen, S. Xie, and K. He, "An empirical study of training self-supervised vision transformers," in *Proc. of IEEE/CVF International Conference on Computer Vision (ICCV)*, 2021.
- [19] M. Caron, H. Touvron, I. Misra, H. Jégou, J. Mairal, P. Bojanowski, and A. Joulin, "Emerging properties in self-supervised vision transformers," in *Proc. of IEEE/CVF International Conference on Computer Vision (ICCV)*, 2021.
- [20] Y. Li, P. Hu, Z. Liu, D. Peng, J. T. Zhou, and X. Peng, "Contrastive clustering," in *Proc. of AAAI Conference on Artificial Intelligence*, 2021.
- [21] Y. Liu, E. Sangineto, W. Bi, N. Sebe, B. Lepri, and M. Nadai, "Efficient training of visual transformers with small datasets," in *Advanced in Neural Information Processing Systems (NeurIPS)*, 2021.
- [22] T. Xiao, M. Singh, E. Mintun, T. Darrell, P. Dollár, and R. Girshick, "Early convolutions help transformers see better," in *Advanced in Neural Information Processing Systems (NeurIPS)*, 2021.
- [23] H. Touvron, M. Cord, M. Douze, F. Massa, A. Sablayrolles, and H. Jégou, "Training data-efficient image transformers & distillation through attention," in *Proc. of International Conference on Machine Learning (ICML)*, 2021.
- [24] Y. Long, Y. Gong, Z. Xiao, and Q. Liu, "Accurate object localization in remote sensing images based on convolutional neural networks," *IEEE Transactions on Geoscience and Remote Sensing*, vol. 55, no. 5, pp. 2486–2498, 2017.
- [25] Y. Yang and S. Newsam, "Bag-of-visual-words and spatial extensions for land-use classification," in *Proc. of SIGSPATIAL International Conference on Advances in Geographic Information Systems*, 2010.
- [26] B. Zhao, Y. Zhong, G.-S. Xia, and L. Zhang, "Dirichlet-derived multiple topic scene classification model for high spatial resolution remote sensing imagery," *IEEE Transactions on Geoscience and Remote Sensing*, vol. 54, no. 4, pp. 2108–2123, 2015.
- [27] G.-S. Xia, J. Hu, F. Hu, B. Shi, X. Bai, Y. Zhong, L. Zhang, and X. Lu, "Aid: A benchmark data set for performance evaluation of aerial scene classification," *IEEE Transactions on Geoscience and Remote Sensing*, vol. 55, no. 7, pp. 3965–3981, 2017.
- [28] C. Xie, R. Wang, J. Zhang, P. Chen, W. Dong, R. Li, T. Chen, and H. Chen, "Multi-level learning features for automatic classification of field crop pests," *Computers and Electronics in Agriculture*, vol. 152, pp. 233–241, 2018.
- [29] M. Cimpoi, S. Maji, I. Kokkinos, S. Mohamed, and A. Vedaldi, "Describing textures in the wild," in *Proc. of IEEE Conference on Computer Vision and Pattern Recognition (CVPR)*, 2014.
- [30] C. Zhu, W. Chen, T. Peng, Y. Wang, and M. Jin, "Hard sample aware noise robust learning for histopathology image classification," *IEEE Transactions on Medical Imaging*, vol. 41, no. 4, pp. 881–894, 2021.
- [31] A. Krizhevsky, G. Hinton *et al.*, "Learning multiple layers of features from tiny images," 2009.
- [32] A. Strehl and J. Ghosh, "Cluster ensembles—a knowledge reuse framework for combining multiple partitions," vol. 3, no. Dec, pp. 583–617, 2002.
- [33] D. Huang, C.-D. Wang, J.-S. Wu, J.-H. Lai, and C.-K. Kwok, "Ultra-scalable spectral clustering and ensemble clustering," vol. 32, no. 6, pp. 1212–1226, 2020.
- [34] D. Huang, C.-D. Wang, J.-H. Lai, and C.-K. Kwok, "Toward multidiversified ensemble clustering of high-dimensional data: From subspaces to metrics and beyond," 2021.
- [35] J. MacQueen *et al.*, "Some methods for classification and analysis of multivariate observations," in *Proc. of Mathematical Statistics and Probability*, 1967.
- [36] L. Zelnik-Manor and P. Perona, "Self-tuning spectral clustering," in *Advanced in Neural Information Processing Systems (NeurIPS)*, 2005.
- [37] K. C. Gowda and G. Krishna, "Agglomerative clustering using the concept of mutual nearest neighbourhood," *Pattern Recognition*, vol. 10, no. 2, pp. 105–112, 1978.
- [38] D. Cai, X. He, X. Wang, H. Bao, and J. Han, "Locality preserving non-negative matrix factorization," in *Proc. of International Joint Conference on Artificial Intelligence (IJCAI)*, 2009.
- [39] A. Martinez and A. Kak, "Pca versus lda," *IEEE Transactions on Pattern Analysis and Machine Intelligence*, vol. 23, no. 2, pp. 228–233, 2001.
- [40] T. Zhang, R. Ramakrishnan, and M. Livny, "BIRCH: An efficient data clustering method for very large databases," in *Proc. of SIGMOD International Conference on Management of Data*, 1996.
- [41] C. Fraley and A. E. Raftery, "Enhanced model-based clustering, density estimation, and discriminant analysis software: MCLUST," vol. 20, no. 2, pp. 263–286, 2003.
- [42] J. Xie, R. Girshick, and A. Farhadi, "Unsupervised deep embedding for clustering analysis," in *Proc. of International Conference on Machine Learning (ICML)*, 2016.
- [43] X. Guo, L. Gao, X. Liu, and J. Yin, "Improved deep embedded clustering with local structure preservation," in *Proc. of International Joint Conference on Artificial Intelligence (IJCAI)*, 2017.
- [44] X. Guo, X. Liu, E. Zhu, X. Zhu, M. Li, X. Xu, and J. Yin, "Adaptive self-paced deep clustering with data augmentation," *IEEE Transactions on Knowledge and Data Engineering*, vol. 32, no. 9, pp. 1680–1693, 2019.
- [45] Y. Tao, K. Takagi, and K. Nakata, "Clustering-friendly representation learning via instance discrimination and feature decorrelation," *arXiv preprint arXiv:2106.00131*, 2021.